arXiv:1003.5927v1 [physics.plasm-ph] 30 Mar 2010

Effects of Line-tying on Magnetohydrodynamic Instabilities and Current Sheet Formation

Yi-Min Huang,[1,2,3,*] A. Bhattacharjee,[1,2,3,†] and Ellen G. Zweibel[4,3,‡]

[1]*Space Science Center, University of New Hampshire, Durham, NH 03824*

[2]*Center for Integrated Computation and Analysis of Reconnection and Turbulence*

[3]*Center for Magnetic Self-Organization in Laboratory and Astrophysical Plasmas*

[4]*Department of Physics and Department of Astronomy, University of Wisconsin, Madison, Wisconsin 53706*

Abstract

An overview of some recent progress on magnetohydrodynamic stability and current sheet formation in a line-tied system is given. Key results on the linear stability of the ideal internal kink mode and resistive tearing mode are summarized. For nonlinear problems, a counterexample to the recent demonstration of current sheet formation by Low *et al.* [B. C. Low and Å. M. Janse, Astrophys. J. **696**, 821 (2009)] is presented, and the governing equations for quasi-static evolution of a boundary driven, line-tied magnetic field are derived. Some open questions and possible strategies to resolve them are discussed.

*Electronic address: yimin.huang@unh.edu

†Electronic address: amitava.bhattacharjee@unh.edu

‡Electronic address: zweibel@astro.wisc.edu

I. INTRODUCTION

In plasma physics, line-tying refers to the presence of conducting walls enclosing the magnetized plasma of interest with a non-vanishing component of the magnetic field normal to the wall. Line-tying is usually employed as an idealization of the boundary condition in some astrophysical plasmas, where the plasma density varies several orders of magnitude over a short distance. For example, the magnetic field lines in the coronae of stars and accretion disks are rooted in the dense, highly conducting gas below. In the limit of infinite density contrast, the dense gas may be treated as a conducting wall at which the field lines are tied.

Line-tying imposes a strong constraint on the plasma motion, therefore in general is stabilizing. This is particularly true in the case of ideal magnetohydrodynamics (MHD). In ideal MHD, magnetic field lines are frozen-in to the plasma flow. If the footpoints of magnetic field lines are not moving, i.e., the wall is rigid, then the footpoint mapping following the field lines from one end to another is conserved. In resistive MHD, magnetic field lines are allowed to slip though the plasma on a resistive time scale. In this sense, the line-tying becomes imperfect, and the stabilizing effect becomes less stringent. It has long been speculated that solar coronal loops can remain stable for longer than typical MHD instability time scale due to line-tying stabilization. [1, 2]

Line-tying may also be used in a broader context with a flow imposed on the boundary, to model the convection on the solar surface or the rotation of accretion disks. The imposed flow shuffles the footpoints of magnetic field lines, twists up and entangles them, thereby converting the kinetic energy of the flow into the magnetic energy in the field. Release of the stored magnetic energy powers some of the most splendid plasma phenomena such as solar flares and coronal mass ejections (CMEs). Dissipation of the magnetic energy on smaller scales is thought to be the energy source of the coronal heating. In a seminal paper, Parker argued that when the magnetic field line topology becomes complicated due to the footpoint shuffling, tangential discontinuities (current sheets) inevitably will form.[3] In the presence of dissipative mechanisms such as resistivity, tangential discontinuities will be smoothed out and the magnetic energy will be turned into heat. Parker coined the term "topological dissipation" to describe this process. Following Parker's original suggestion, many authors [4–9] have shown by direct numerical simulation that random shuffling of

the coronal magnetic field lines by photospheric motions progressively increases the current density, resulting in sporadic energy release.

The key ingredient of Parker's scenario of coronal heating is the ubiquitous presence of current sheets in a magnetized plasma. To illustrate his point, Parker considered a uniform magnetic field $B_0\hat{\mathbf{z}}$ line-tied to conducting plates at $z = \pm L/2$, which represent the photosphere. Motions in the photosphere displace the field-line footpoints and entangle the field lines. Suppose we freeze the footpoints and let the system relax to the minimum energy state under the condition of preserving all the ideal topological constraints. Parker argues that in general the minimum energy state must contain tangential discontinuities. Since its first appearance in Ref. [3], this simple setting has become the "standard model" of the Parker problem. The property that magnetostatic equilibria tend to form tangential discontinuities is stated as a "Magnetostatic Theorem" in Parker's book.[10] Although Parker gives compelling physical arguments in support of the Theorem, no rigorous proof is given.

Parker's claim has stimulated considerable debate that continues to this day[11–17], without apparent consensus. The point of contention is whether or not a magnetic field with neither null points, nor separatrices, nor closed field lines can develop tangential discontinuities. It is well established that null points, separatrices, or closed field lines are the preferential sites for current sheet formation when a system undergoes some instabilities or is deformed via boundary conditions.[18–24] In the Parker problem, however, none of these structures are present. Van Ballegooijen was the first to question Parker's claim. He demonstrated by an analytical argument that the equilibrium will always be continuous, unless the footpoint mapping is discontinuous.[11, 25] Subsequently, several authors have found smooth equilibria using either linear theories for small footpoint displacements or Lagrangian numerical relaxation schemes for nonlinear problems. [12, 16, 17, 26] However, as pointed out by Ng and Bhattacharjee,[15] van Ballegooijen's argument is valid only for simple current sheets; it fails if a current sheet has multiple branches joined together (see Figure 2 of Ref. [15]). Ng and Bhattacharjee also proved a theorem which asserts that there is at most one smooth equilibrium for any given smooth footpoint mapping. It follows that if a smooth equilibrium becomes unstable, there is no other smooth equilibrium the system can relax to; therefore the system must relax to an equilibrium with tangential discontinuities. The theorem of Ng and Bhattacharjee is within the framework of reduced magnetohydrodynamics (RMHD), which assumes the existence of a strong guide field.[27, 28] It also assumes double-

periodicity in the plane perpendicular to the guide field. It is not known at the present time whether the result can be generalized to full MHD or more general boundary conditions, although Aly [29] appears to have taken an important step towards that goal. Lagrangian relaxation studies indeed suggest current sheet may form under certain circumstances,[16, 17] although it is rather difficult to draw decisive conclusions from numerical studies due to limits of spatial resolution.

This paper gives an overview of our recent progress on MHD stability and current sheet formation in a line-tied system. Previously published results are summarized in Sec. II and Sec. III, with new perspectives added. Sec. II summarizes the results on linear stability regarding line-tying effects on the ideal internal kink mode and resistive tearing mode. Parker's problem on current sheet formation is discussed in Sec. III. The discussion is divided into two parts. The first part discusses why the nonlinear evolution of ideal kink mode is a relevant setting to test Parker's hypothesis. The second part is a discussion about the recent demonstration of current sheet formation by Low *et al.* [30–33] and our objection to it.[34] Some outstanding open questions will be discussed along the way. Sec. IV contains the new results, where the governing equations for quasi-static evolution of a boundary driven, line-tied magnetic field are derived, and a possible strategy of applying these equations to fully settle an open question regarding the Parker problem as well as the demonstration of Low *et al.* is outlined. Finally, some future perspectives are discussed in Sec. V.

II. LINE-TYING EFFECTS ON IDEAL AND RESISTIVE MHD INSTABILITIES

A. Ideal Internal Kink Mode

A line-tied screw pinch is often employed as a model of solar coronal loops. Assuming that the plasma pressure is negligible, in cylindrical coordinates (r, ϕ, z), the equilibrium magnetic field is

$$\mathbf{B} = B_\phi(r)\hat{\boldsymbol{\phi}} + B_z(r)\hat{\mathbf{z}}, \tag{1}$$

which satisfies the force balance equation

$$-\frac{d}{dr}\left(\frac{B^2}{8\pi}\right) - \frac{B_\phi^2}{4\pi r} = 0. \tag{2}$$

In a periodic pinch of length L, we may decompose the plasma displacement $\boldsymbol{\xi}$ into Fourier basis in both z and ϕ directions. Therefore we consider an eigenmode of the form $\boldsymbol{\xi} = \boldsymbol{\xi}(r)e^{\gamma t+i(kz+m\phi)}$, where $k = 2n\pi/L$, γ is the growth rate, and both n and m are integers. The $m = \pm 1$ internal kink mode is unstable if the safety factor $q \equiv 2\pi r B_z/LB_\phi$ drops below unity within the plasma and increases with radius. Unstable modes have helical symmetry, depending on z and ϕ in the combination $kz \pm \phi$, and possess a so-called resonant surface $r = r_s$, on which $\mathbf{k}\cdot\mathbf{B} = kB_z \pm B_\phi/r_s = 0$. Due to the constraint of periodicity, the resonant surface must also be a rational surface on which magnetic field lines are closed. The driver of the instability lies within r_s, and the radial component of the plasma displacement nearly vanishes outside it. It has been shown that the thin transition layer near r_s predicted from linear theory corresponds to an infinite current sheet in finite amplitude theory, at least within the framework of reduced, ideal MHD.[19, 35] In a line-tied pinch, the boundary condition constrains the plasma displacement $\boldsymbol{\xi}$ to zero at $z = \pm L/2$. Therefore a Fourier decomposition can no longer be done in z, and the eigenvalue problem is inherently two-dimensional (2D). At a fundamental level, there is a deeper issue. In a line-tied screw pinch, all magnetic field lines are topologically equal; they all go from one end plate to another (assuming $B_z \neq 0$ everywhere). Therefore the notions of rational surfaces and resonant surfaces are no longer valid. A question is: is there still a steep gradient in the eigenmode, as in the periodic counterpart? And if the answer is yes, where will the steep gradient be?

In Ref. [36] a detailed study of the line-tied internal kink mode has been carried out. It was found that the fastest growing internal kink mode in a line-tied system possesses a steep internal layer. The internal layer is located at the resonant surface of the fastest growing periodic mode in an *infinitely* long system (i.e., k is a continuum). However, the internal layer in a line-tied system is smoother than its periodic counterpart. Only in the limit $L \to \infty$ does the former approaches the latter. This can be seen in Figure 1, which shows the radial displacement ξ_r and parallel current $J_\parallel$ of eigenmodes for different L along the midplane $z = 0$, as compared to its periodic counterparts. Similar results have been found in Refs. [37, 38] for different equilibria and Ref. [39] including finite pressure effects.

There is a critical length L_c for the instability. When $L < L_c$ the internal kink is stabilized. The critical length L_c is approximately given by

$$L_c \simeq 2\left|V_{Az}\right|_{r_s}/\gamma_0, \tag{3}$$

where γ_0 and r_s are the growth rate and the resonant surface of the fastest growing periodic mode, respectively, and V_{Az} is the z component of the Alfvén speed. This is roughly consistent with the heuristic stability criterion that the unstable mode is stabilized when the Alfvén transit time along the loop is less than the inverse of the growth rate in a periodic system. Once the critical length L_c is known, the growth rate γ for a system of length L can be determined by solving the equation

$$\frac{L_c}{L} = \frac{\gamma/\gamma_0}{\tanh^{-1}(\gamma/\gamma_0)}. \tag{4}$$

In the limit $L \to \infty$, the growth rate $\gamma \to \gamma_0$. The growth rate γ_0 in a periodic pinch scales as

$$\gamma_0 \sim \epsilon^3 \left| V_{Az} \right| / a, \tag{5}$$

where a is the characteristic radius of the pinch and $\epsilon \sim B_\phi/B_z$ is the tilt angle, which typically is a smaller parameter. The critical length $L_c \sim a/\epsilon^3$. In solar applications, often the coronal loop length and the axial field B_z are given, and the azimuthal component B_ϕ is generated by applying some footpoint twisting. Then we can ask the following question: what is the critical twisting angle ϕ_c for the loop to become unstable? From $L_c \sim a/\epsilon^3$ we have the critical tilt angle $\epsilon_c \sim (a/L)^{1/3}$ when L is given. That corresponds to a critical twisting angle

$$\phi_c \sim \frac{L}{a}\epsilon_c \sim \left(\frac{L}{a}\right)^{2/3}. \tag{6}$$

The precise value of the critical tilt angle ϵ_c depends on the profile. For the profile $B_\phi = \text{const} \times (r/a)\exp(-(r/a)^2)$, which was considered in Ref. [36], the critical tilt angle at $r = a$ is approximately given by

$$\epsilon_c \simeq 1.1 \times \left(\frac{a}{L}\right)^{1/3}. \tag{7}$$

The critical tilt angle depends on the aspect ratio (a/L) rather weakly. For a coronal loop with $a/L = 1/100$, the critical tilt angle $\epsilon_c \simeq 0.24$, which is approximately 14°. For a shorter loop with $a/L = 1/10$, the critical tilt angle is about 29°; whereas for an extremely long loop with $a/L = 1/1000$, the critical tilt angle is about 6.3°. These numbers are in reasonable agreement with estimates obtained from balancing the Poynting flux from the coronal base and the observed coronal loss rate, which give a tilt angle ranging from 10° to 20°.[40, 41]

B. Resistive Tearing Mode

When a small but finite resistivity η is included in the theory, line-tying becomes imperfect. In Ref. [42], Delzanno *et al.* studied the resistive effects on line-tied internal kink modes. They found that when the system length L is greater than the ideal critical length L_c^{ideal}, the mode growth rate is similar to the ideal one. However, resistivity can make a system with $L < L_c^{ideal}$ unstable. Interestingly, the critical length of a resistive system L_c^{res} is found to be independent of η.

In Ref. [43], we studied the effects of line-tying on the resistive tearing instability in slab geometry. The equilibrium has a strong guide field B_z along z, and B_y changes direction across a current layer around $x = 0$. Two conducting plates at $z = \pm L/2$ provide the line-tied boundary condition. This configuration is ideally stable, but can be unstable to the tearing mode when $\eta > 0$. The instability is studied within the framework of the RMHD equations.[28, 44] After proper normalization, the magnetic field and the velocity can be expressed in terms of the flux function ψ and the stream function ϕ as $\mathbf{B} = \hat{\mathbf{z}} + \nabla_\perp \psi \times \hat{\mathbf{z}}$ and $\mathbf{u} = \nabla_\perp \phi \times \hat{\mathbf{z}}$. The governing equations are

$$\partial_t \Omega + [\phi, \Omega] = \partial_z J + [\psi, J] \,, \tag{8}$$

Here $\nabla_\perp \equiv \hat{\mathbf{x}}\partial_x + \hat{\mathbf{y}}\partial_y$ is the perpendicular gradient; $\Omega = -\nabla_\perp^2 \phi$, $J = -\nabla_\perp^2 \psi$ are the vorticity and the electric current; and $[\psi, \phi] \equiv \partial_y \psi \partial_x \phi - \partial_x \psi \partial_y \phi$ is the Poisson bracket. The standard Harris sheet $B_y = \text{const} \times \tanh x$, is assumed, but more general profiles can be easily implemented.

In a periodic system, we may consider linear perturbations of the form $\tilde{\phi} = \tilde{\phi}(x) e^{\gamma t + i k_y y + i k_z z}$ and $\tilde{\psi} = \tilde{\psi}(x) e^{\gamma t + i k_y y + i k_z z}$. The system is unstable to the tearing mode with a growth rate $\gamma \sim \eta^{3/5}$ in the asymptotic limit $\eta \to 0$. With line-tying, Fourier decomposition along z is not possible and a two-dimensional eigenvalue problem has to be solved. In this case, the system is unstable only when L is greater than a critical length L_c, which is found to be independent of η. However, near marginal stability, the linear unstable mode grows slowly, and plasma inertia can be neglected everywhere. With this "force-free" approximation, the growth rate γ is proportional to η. When L is sufficiently long, plasma inertia can no longer be neglected within the resistive layer. In this regime, the line-tied growth rate approaches the periodic one, and the $\gamma \sim \eta^{3/5}$ scaling is recovered. The transi-

tion from the force-free regime to the inertia dominated regime occurs at a transition length L_t which scales as $L_t \sim \eta^{-2/5}$. Notice that without line-tying, the force-free approximation only applies in the outer region; in the resistive layer, plasma inertia (or viscosity) has to be included, otherwise the equations become singular at the resonant surface where $\mathbf{k} \cdot \mathbf{B} = 0$. In a line-tied system, on the other hand, it is possible that the force-free approximation is applicable over the whole domain, provided that the mode grows slowly. This is because that there is no resonant surface in a line-tied system, and the equations are not singular even without plasma inertia. The resistive layer persists even with line-tying. However, line-tying effects make the resistive layer smoother; when the system length L becomes longer, the resistive layer becomes steeper. This general trend, as shown in Figure 2, resembles that in the internal layer of the ideal internal kink mode. Similar results have been found in cylindrical geometry by Delzanno *et al.* [45]

III. CURRENT SHEET FORMATION AND THE PARKER PROBLEM

A. Nonlinear Saturation of the Ideal Kink in Line-tied Geometry

A question that remains open is the nonlinear saturation of ideal internal kink mode in a line-tied screw pinch. After the onset of the instability, if we let the magnetic field relax to a minimum energy state but preserve all the ideal topological constraints, will it develop a tangential discontinuity? This is an excellent setting for testing Parker's conjecture, as the initial condition contains neither null points nor separatrices nor closed field lines. In a periodic pinch the answer to the question is yes, as shown by Rosenbluth *et al.* that a helical ribbon-like current sheet will form at the resonant surface, which is also a rational surface.[19, 35] In a line-tied system, the answer is not so clear. The steep gradient in the line-tied eigenfunction (Figure 1) suggests that a thin current filament will form. Indeed, a helical thin current filament has been observed in several nonlinear simulations. [46–51] However, whether it is a current singularity or not is very difficult to settle by a numerical calculation. We have seen that line-tying in general has the effect of smoothing out the internal layer of the linear eigenmode; it may have a similar effect to the nonlinear saturation and turn a current singularity into a thin current layer with a finite width. If this turns out to be the case, we may expect the current layer to become thinner as the system length

becomes longer, assuming that the equilibrium profile remains unchanged.

The theorem of Ng and Bhattacharjee, as discussed in the Introduction, asserts that if a smooth equilibrium becomes unstable, the system must relax to an equilibrium with tangential discontinuity. According to the theorem, it appears that the ideal internal kink mode will develop a current sheet. However, the theorem does not apply to the present case for the following reasons. First, the theorem is proved within the framework of RMHD, in which the ideal internal kink mode is marginally stable. To capture the internal kink mode one has to carry out the expansion to higher orders. This also raises the question whether the theorem can be generalized to full MHD or not, as some unstable modes are clearly missing in RMHD. Second, the proof assumes double periodicity in the perpendicular plane, and a screw pinch does not belong to this category.

B. A Counterexample to the Demonstration of Current Sheet Formation by Low *et al.*

Recently, in a series of papers [30–33], Low and coauthors have tried to demonstrate unambiguously the formation of current singularities using what they call "topologically untwisted fields", which, in the context of force-free fields, is synonymous with potential fields. That is, they limit themselves to a special subset of force-free fields which contains no electric current. In this case, the magnetic field can be expressed as $\mathbf{B} = \nabla\chi$ with some potential χ, where χ satisfies $\nabla^2\chi = 0$ because $\mathbf{B}$ is divergenceless. In a simply connected, compact domain, χ is uniquely determined up to an additive constant if the normal derivative of χ is specified on the boundary. Therefore, a potential field is uniquely determined by prescribing the normal component of $\mathbf{B}$ ($= \hat{\mathbf{n}}\cdot\nabla\chi$, where $\hat{\mathbf{n}}$ is the unit normal vector) on the boundary. In Ref. [32], the authors consider a potential field in a cylinder of finite length as an initial condition; the normal component of the field is nonzero only at the top and the bottom of the cylinder. The cylinder is then compressed to a shorter length. Because the whole process is governed by the ideal induction equation, the normal component of the field remains the same. By making a *key assumption* that the field will remain potential during the process, they circumvent the complicated problem of solving for the various stages of quasi-static evolution, and simply calculate the magnetic field in the final state as the potential field which satisfies the boundary conditions. They then

numerically calculate the magnetic field line mapping from one end to the other, for both the initial and the final states. They find that for a three-dimensional (3D) field, the field line mapping, and hence, the topology, is changed. Because an ideal evolution preserves the magnetic topology, the authors claim that the field must evolve into a state which contains tangential discontinuities; furthermore, singularities may form densely due to the ubiquitous change of the field line mapping.

The assumption that the field will remain potential during the compression, however, is not proven in their work. The reasoning behind the assumption could be understood as follows. Consider a magnetic field line (the base field line) and a neighboring field line which is infinitesimally separated from it. As we follow along the field lines, in general the neighboring field line winds around the base field line at a rate $d\phi/ds \neq 0$, where s is the arc length along the field line and ϕ is the azimuthal angle of the displacement vector between the two field lines relative to a comoving reference frame. Here the comoving reference frame is specified by three mutually perpendicular vectors at each point along the field line. One of the vectors is tangent to the field line, while the other two follow parallel transport along the field line. (See Appendix A for the detail of how parallel transport is defined. One also should not confuse the azimuthal angle ϕ here with the angle of rotational transform in a toroidal device, where the base field line is a closed loop. For the rotational transform, the well-known Frenet-Serret frame is a good reference frame. The Frenet-Serret frame does not follow parallel transport in case the base field line has a nonvanishing torsion. See Appendix A for further discussion.) In general, different neighboring field lines have different winding rates. However, for a force-free field satisfying

$$\nabla \times \mathbf{B} = \lambda \mathbf{B} \tag{9}$$

with $\mathbf{B} \cdot \nabla \lambda = 0$, it can be shown that the averaged local winding rate over all neighboring field lines is related to λ as (see Appendix A for a derivation)

$$\left\langle \frac{d\phi}{ds} \right\rangle = \frac{\lambda}{2}. \tag{10}$$

This simple relation shows that parallel current is related to the winding between neighboring field lines. For a potential field, which satisfies $\lambda = 0$ everywhere, the average local winding rate $\langle d\phi/ds \rangle$ is equal to zero. This justifies the use of the term "untwisted fields" for potential fields. Intuitively, it would appear to require a nonzero vorticity on the boundary,

which is absent in a simple expansion or compression, to twist up the field. Therefore, it is plausible that a potential field will remain potential during a simple expansion or compression. However, in Ref. [34], an explicit counterexample is constructed in a two-dimensional (2D) slab geometry. The counterexample demonstrates that a potential field can evolve to a smooth, non-potential field under simple expansion or compression. The construction is summarized as follows.

Consider a 2D configuration in Cartesian geometry, with x the direction of symmetry. A general magnetic field may be expressed as

$$\mathbf{B} = B_x \hat{\mathbf{x}} + \hat{\mathbf{x}} \times \nabla \psi, \tag{11}$$

where $B_x = B_x(y, z)$ and $\psi = \psi(y, z)$. For a force-free field, $B_x = B_x(\psi)$ and ψ must satisfy the Grad-Shafranov equation

$$\nabla^2 \psi = -B_x \frac{dB_x}{d\psi}, \tag{12}$$

where λ in Eq. (9) is equal to $-dB_x/d\psi$ in this representation. If the field is potential, then $B_x = \text{const}$ and $\nabla^2 \psi = 0$.

Let us consider a force-free field bounded by two conducting surfaces at $z = 0$ and $z = L$, with all field lines connecting one end plate to the other. The footpoint mapping from one end to the other is characterized by ψ on the boundaries, as well as the axial displacement along x when following a field line from the bottom to the top:

$$h(\psi) = B_x(\psi) \left(\int_{z=0}^{z=L} \frac{1}{|\nabla \psi|} ds \right)_\psi . \tag{13}$$

Here ds is the line element on the $y - z$ plane, and the subscript ψ indicates that the integration is done along a constant ψ contour.

Let the initial condition be (B_{x0}, ψ_0) with a system length L_0. Suppose the system has undergone a simple expansion or compression such that the system length changes to some $L \neq L_0$. Since ideal evolution preserves the footpoint mapping, the flux function ψ on the boundaries and the axial displacement $h(\psi)$ must remain unchanged. To determine the final force-free equilibrium, we must solve the two coupled equations

$$\nabla^2 \psi = -B_x \frac{dB_x}{d\psi}, \tag{14}$$

and

$$B_x(\psi) = h(\psi) \left(\int_{z=0}^{z=L} \frac{1}{|\nabla\psi|} ds \right)_{\psi}^{-1}, \tag{15}$$

subject to the conditions $\psi(y,0) = \psi_0(y,0)$, $\psi(y,L) = \psi_0(y,L_0)$, where the axial displacement $h(\psi)$ is determined from the initial condition. The set of coupled equations (14) and (15) is called a generalized differential equation, which in general requires numerical solutions. [52]

In Ref. [34], we consider the initial condition $\psi_0 = y + \epsilon \sin(y) \cosh(z - 1/2)$, $B_{x0} = 1$, and $L_0 = 1$, where $\epsilon \ll 1$ is a small parameter. Eqns. (14) and (15) are solved for arbitrary L both analytically with a perturbation theory and numerically. The results from both approaches are consistent, and the final state is found to be smooth, but contains non-vanishing current, and is therefore non-potential.

It should be pointed out that our configuration is not within a compact domain. Furthermore, the example we worked out is periodic along the y direction, even though that is not required by the formalism. Topologically, the geometry is equivalent to the space between two concentric, infinitely long cylinders, therefore not simply connected.[53] Consequently, specifying the normal component of the magnetic field on the boundary does not uniquely determine the potential field. One can, for example, add a constant B_y or B_x to the field without changing the normal component of $\mathbf{B}$. In this regard, our configuration does not belong to the same class of configurations considered by Low *et al.* Nevertheless, our example shows that the demonstration by Low *et al.* is not complete if their key assumption is not proven. Another criticism of the demonstration of Low *et al.* has been raised recently by Aly and Amari from a different point of view.[54] To fully settle the issue in the future, a more general formalism for the quasi-static evolution of a boundary driven magnetic field is needed. This is the topic of the next section.

IV. QUASI-STATIC EVOLUTION OF A BOUNDARY DRIVEN LINE-TIED MAGNETIC FIELD

The governing equation for quasi-static evolution driven by boundary motions was derived by van Ballegooijen (VB) [11] within the framework of RMHD. This is under the assumption that the characteristic time scales of the boundary motions are much longer compared to the Alfvén transit times, therefore the system remains force-free for all time to a good

approximation. Here we generalize the VB equation to full MHD without assuming any asymptotic ordering.

We assume that the system satisfies the force-free condition (9) for all time. The magnetic field evolves according to the ideal induction equation

$$\partial_t \mathbf{B} = -\nabla \times \mathbf{E} = \nabla \times (\mathbf{u} \times \mathbf{B}), \tag{16}$$

where $\mathbf{u}$ is the plasma flow and $\mathbf{E}$ the electric field. Now suppose the magnetic field $\mathbf{B}$ and the boundary velocity $\mathbf{u}^b$ are given at $t = t_0$. The objective is to find a plasma flow $\mathbf{u}$ which is consistent with the prescribed boundary flow $\mathbf{u}^b$, and which, when evolving the magnetic field according to the ideal induction equation (16), carries the system to a neighboring force-free equilibrium at $t = t_0 + dt$. Following VB, first we take the time derivative of the force-free condition (9). This yields

$$\nabla \times \partial_t \mathbf{B} = \mathbf{B}\partial_t \lambda + \lambda \partial_t \mathbf{B}. \tag{17}$$

Using the induction equation (16) and $\mathbf{B} \cdot \nabla \lambda = 0$, Eq. (17) may be rewritten as

$$\begin{aligned} \frac{d\lambda}{dt}\mathbf{B} &= (\partial_t \lambda + \mathbf{u} \cdot \nabla \lambda)\, \mathbf{B} = \nabla \times (\lambda \mathbf{E} - \nabla \times \mathbf{E}) \\ &= -\nabla \times (\lambda \mathbf{u} \times \mathbf{B} - \nabla \times (\mathbf{u} \times \mathbf{B})). \end{aligned} \tag{18}$$

Taking the divergence of Eq. (18) yields

$$\mathbf{B} \cdot \nabla \frac{d\lambda}{dt} = 0, \tag{19}$$

which is consistent with the condition that $\mathbf{B} \cdot \nabla \lambda = 0$ is satisfied for all time. Equation (18) is the equivalent of the VB equation in the framework of full MHD. It has to be solved for $\mathbf{u}$ subject to the boundary condition prescribed by the boundary flow $\mathbf{u}^b$. In other words, we have to find a flow $\mathbf{u}$ such that $\nabla \times (\lambda \mathbf{u} \times \mathbf{B} - \nabla \times (\mathbf{u} \times \mathbf{B}))$ is proportional to $\mathbf{B}$ everywhere inside the domain. Clearly only the component of $\mathbf{u}$ perpendicular to $\mathbf{B}$, $\mathbf{u}_\perp$, can be determined from this approach. The parallel component $u_\parallel$ is arbitrary, except that it has to be consistent with the boundary condition. Equation (18) may be solved for very general boundary conditions, including convection ($\mathbf{u}^b \cdot \hat{\mathbf{n}} = 0$), expansion or compression ($\mathbf{u}^b \times \hat{\mathbf{n}} = 0$), or a combination of both. If the trajectory of each boundary point is prescribed, solving Eq. (18) at each instance and integrating Eq. (16) at the same time will carry the magnetic field through a series of force-free equilibria. Notice that Eq. (18) is linear in

$\mathbf{u}$ at each instant of time. That is, if $(d\lambda_1/dt; \mathbf{u}_1)$ is a solution for the boundary flow $\mathbf{u}_1^b$ and $(d\lambda_2/dt; \mathbf{u}_2)$ a solution for $\mathbf{u}_2^b$, then $(c_1 d\lambda_1/dt + c_2 d\lambda_2/dt, c_1\mathbf{u}_1 + c_2\mathbf{u}_2)$ is a solution $\mathbf{u}^b = c_1\mathbf{u}_1^b + c_2\mathbf{u}_2^b$, where c_1 and c_2 are arbitrary constants.

The time evolution of λ is of particular interest here. It allows us to address the issue regarding Low's assumption. Starting from a potential field, i.e., $\lambda = 0$ everywhere, Eq. (18) becomes

$$\frac{d\lambda}{dt}\mathbf{B} = \nabla \times \nabla \times (\mathbf{u} \times \mathbf{B})\,. \tag{20}$$

The field will remain potential if $d\lambda/dt = 0$ everywhere. Therefore, it will be sufficient to take the initial condition of Low *et al.*, and solve Eq. (20). The boundary conditions can be chosen as $\mathbf{u}^b_{top} = \hat{\mathbf{z}}$, $\mathbf{u}^b_{bottom} = 0$, and $\mathbf{u}^b_{side}$ varies continuously from the bottom to the top and matches the velocity at the bottom and the top. If the solution turns out to have $d\lambda/dt \neq 0$, then the assumption of Low *et al.* is disproved. On the other hand, if Eq. (20) does not have a smooth solution, then current singularities will form immediately. A third possibility is that a smooth solution exists, and satisfies $d\lambda/dt = 0$. In this case we have to follow the time evolution through a series of potential fields until either one of the previous two possibilities is realized. (The field cannot remain a smooth potential field forever, as this contradicts the findings of Ref. [33].) If Low *et al.* are indeed correct, this approach may answer the questions regarding when, and where current singularities will form. It is not difficult to see that in general $d\lambda/dt$ will not be zero, as follows. The solution to Eq. (20) determines the components of $\mathbf{u}$ perpendicular to $\mathbf{B}$; that is, there are two degrees of freedom at each point. And Eq. (20) demands that $\nabla \times \nabla \times (\mathbf{u} \times \mathbf{B})$ be parallel to $\mathbf{B}$, which again corresponds to two independent constraints at each point. Therefore we have the same number of unknowns and equations. If the magnetic field is to remain potential, then the condition $(\nabla \times \nabla \times (\mathbf{u} \times \mathbf{B}))_{\|} = 0$ should be satisfied as well. This would correspond to a third independent constraint at each point, and the system is then overdetermined. Of course, the boundary motion considered by Low *et al.* is a very special one. Therefore we cannot preclude the possibility that in their case $\nabla \times \nabla \times (\mathbf{u} \times \mathbf{B}) \parallel \mathbf{B}$ implies $\nabla \times \nabla \times (\mathbf{u} \times \mathbf{B}) = 0$, when the solution is smooth. If this can be proven to be the case, then the assumption of Low *et al.* is proven.

The approach outlined here has been applied to the example described in Sec. III B. And indeed the solution of Eq. (20) has $d\lambda/dt \neq 0$, consistent with our findings from the approach mentioned in Sec. III B that the field will evolve into a non-potential field. A

similar approach has been taken by Scheper and Hassam in their demonstration of current sheet formation in 2D slab geometry, for an initial field with separatrices.[24] The initial condition of Low *et al.* is fully 3D, therefore solving Eq. (20) is more difficult, requiring numerical treatment.

V. FUTURE PERSPECTIVES

In this paper, we have reviewed some of the recent progress regarding the effects of line-tying on MHD instabilities and current sheet formation and presented some new results. For the problems of linear stability, it is shown that line-tying in general has a stabilizing effect. Furthermore, because of the absence of a resonant surface in a line-tied system, the internal layer of the eigenfunction, although it persists, is smoother than its periodic counterpart. For the more important nonlinear problems, there remain two outstanding questions: the nonlinear saturation of the line-tied ideal internal kink mode and the complete resolution of the issue regarding the assumption made by Low *et al.* in their demonstration of current singularities. These open questions pose significant challenges for the future, involving analysis as well as numerical computation. The nonlinear saturation of the internal kink mode may be attacked by some numerical force-free field solvers that preserve the field line topology, such as Lagrangian relaxation schemes.[16, 17, 55] If the final equilibrium has a thin, but non-singular current layer, it may be fully resolved with convergence, provided that the resolution is sufficient. For the second question, a possible approach is outlined in Sec. IV, by solving the derived governing equations for a quasi-static, boundary driven magnetic field. Another possible approach is solving the final equilibrium of the compressed system by a force-free field solver, mentioned above. In any case, we are facing a problem where the solution may become singular, therefore a reliable mean to ascertain singularities numerically may be needed.

The formalism derived in Sec. IV also opens up the possibility of generalizing the proof of Ng and Bhattacharjee, which relies heavily on the VB equation, to full MHD. This will be a topic of future investigation.

Acknowledgments

This research is supported by the National Science Foundation, Grant No. PHY-0215581 (PFC: Center for Magnetic Self-Organization in Laboratory and Astrophysical Plasmas) and the Department of Energy, Grant No. DE-FG02-07ER46372, under the auspice of the Center for Integrated Computation and Analysis of Reconnection and Turbulence (CICART).

Appendix A: Comoving Frame of Reference, Parallel Transport, and a Derivation of Eq. (10)

Let $\mathbf{X}(s)$ be a magnetic field line (the "base" field line) parameterized by the arc length s. A comoving reference frame along the magnetic field line is specified by three mutually perpendicular unit vectors $\{\mathbf{e}_1(s), \mathbf{e}_2(s), \mathbf{e}_3(s)\}$ at each point along the field line. Here we further require $\mathbf{e}_3$ to be the tangent vector. That is, $\mathbf{e}_3 = d\mathbf{X}/ds = \hat{\mathbf{b}} = \mathbf{B}/B$. In general, the basis vectors $\{\mathbf{e}_i\}_{i=1,2,3}$ follow

$$\frac{d\mathbf{e}_i}{ds} = \boldsymbol{\omega} \times \mathbf{e}_i, \tag{A1}$$

where $\boldsymbol{\omega}$ can be regarded as the angular "velocity", if we treat the arc length s as the time variable. We adopt the following definition of parallel transport: a comoving frame is said to be parallelly transported along a field line if the angular velocity is perpendicular to the magnetic field. That is, the angular velocity satisfies $\boldsymbol{\omega} \cdot \mathbf{e}_3 = 0$. Under this condition, the comoving frame is not rotating with respect to the direction of the magnetic field, therefore is a good reference frame for measuring the local winding rate of neighboring field lines. From $d\mathbf{e}_3/ds = \boldsymbol{\omega} \times \mathbf{e}_3$ and $\boldsymbol{\omega} \cdot \mathbf{e}_3 = 0$, the angular velocity is uniquely determined as

$$\boldsymbol{\omega} = \mathbf{e}_3 \times \frac{d\mathbf{e}_3}{ds}. \tag{A2}$$

If a set of basis vectors is given at one point, then the comoving frame following parallel transport at each point can be obtained by integrating Eq. (A1) with the angular velocity given by Eq. (A2). Specifically,

$$\frac{d\mathbf{e}_1}{ds} = -\left(\mathbf{e}_1 \cdot \frac{d\mathbf{e}_3}{ds}\right)\mathbf{e}_3, \tag{A3}$$

$$\frac{d\mathbf{e}_2}{ds} = -\left(\mathbf{e}_2 \cdot \frac{d\mathbf{e}_3}{ds}\right)\mathbf{e}_3. \tag{A4}$$

Having set up the comoving frame, we can now define a local coordinate system (a_1, a_2, s) in a neighborhood of the field line:

$$\mathbf{x}(a_1, a_2, s) = \mathbf{X}(s) + a_1\mathbf{e}_1 + a_2\mathbf{e}_2. \tag{A5}$$

Now suppose there is a neighboring field line with a trajectory defined by $\mathbf{X}'(s) = \mathbf{X}(s) + \delta\mathbf{x}(s) = \mathbf{X}(s) + a_1(s)\mathbf{e}_1 + a_2(s)\mathbf{e}_2$, where a_1 and a_2 are infinitesimal. The differential arc length of the neighboring field line $\mathbf{X}'(s)$ is

$$ds' = \sqrt{\frac{d\mathbf{X}'}{ds} \cdot \frac{d\mathbf{X}'}{ds}} ds = \left(1 - \delta\mathbf{x} \cdot \frac{d\mathbf{e}_3}{ds}\right) ds, \tag{A6}$$

where Eqs. (A3) and (A4) are applied. The magnetic field at $\mathbf{X}'(s)$ is

$$\mathbf{B}'(s) = B(s)\mathbf{e}_3 + \delta\mathbf{x} \cdot \nabla\mathbf{B}, \tag{A7}$$

which has a magnitude

$$B'(s) = B(s) + \mathbf{e}_3 \cdot (\delta\mathbf{x} \cdot \nabla\mathbf{B}). \tag{A8}$$

Using Eqs. (A6), (A7), and (A8) in the field line equation $d\mathbf{X}'/ds' = \mathbf{B}'/B'$ yields the governing equation for $\delta\mathbf{x}$:

$$\left(\frac{d}{ds}\delta\mathbf{x}\right)_\perp = \frac{1}{B(s)} (\delta\mathbf{x} \cdot \nabla\mathbf{B})_\perp, \tag{A9}$$

where the subscript $\perp$ indicates a projection onto the plane spanned by $\mathbf{e}_1$ and $\mathbf{e}_2$. Equation (A9) can be written explicitly as

$$\frac{d}{ds}\begin{bmatrix} a_1 \\ a_2 \end{bmatrix} = M(s)\begin{bmatrix} a_1 \\ a_2 \end{bmatrix}, \tag{A10}$$

where

$$M(s) = \frac{1}{B(s)}\begin{bmatrix} (\nabla\mathbf{B})_{11} & (\nabla\mathbf{B})_{21} \\ (\nabla\mathbf{B})_{12} & (\nabla\mathbf{B})_{22} \end{bmatrix}, \tag{A11}$$

and

$$(\nabla\mathbf{B})_{ij} \equiv (\mathbf{e}_i \cdot \nabla\mathbf{B}) \cdot \mathbf{e}_j. \tag{A12}$$

The winding rate of the neighboring field line becomes apparent if we express the deviation $\delta\mathbf{x}$ in terms of the local polar coordinates (r, ϕ), which are related to (a_1, a_2) by $a_1 = r\cos\phi$ and $a_2 = r\sin\phi$. It follows from Eq. (A10) that

$$\frac{1}{r}\frac{dr}{ds} = \frac{1}{B(s)}\left((\nabla\mathbf{B})_{11}\cos^2\phi + \frac{(\nabla\mathbf{B})_{12}+(\nabla\mathbf{B})_{21}}{2}\sin 2\phi + (\nabla\mathbf{B})_{22}\sin^2\phi\right), \tag{A13}$$

and

$$\frac{d\phi}{ds} = \frac{1}{B(s)}\left(\frac{(\nabla\mathbf{B})_{22}-(\nabla\mathbf{B})_{11}}{2}\sin 2\phi + (\nabla\mathbf{B})_{12}\cos^2\phi - (\nabla\mathbf{B})_{21}\sin^2\phi\right). \tag{A14}$$

Equation (A13) determines whether the two field lines are diverging from or converging towards each other, and Eq. (A14) gives the winding rate $d\phi/ds$ of the neighboring field line with respect to the base field line. Clearly, $d\phi/ds$ depends on ϕ. Therefore, in general different neighboring field lines have different winding rates. Averaging Eqs. (A13) and (A14) over ϕ yields

$$\left\langle\frac{1}{r}\frac{dr}{ds}\right\rangle = \frac{1}{2B(s)}\left((\nabla\mathbf{B})_{11}+(\nabla\mathbf{B})_{22}\right) = -\frac{1}{2B}\frac{dB}{ds}, \tag{A15}$$

and

$$\left\langle\frac{d\phi}{ds}\right\rangle = \frac{1}{2B(s)}\left((\nabla\mathbf{B})_{12}-(\nabla\mathbf{B})_{21}\right) = \frac{\mathbf{e}_3\cdot\nabla\times\mathbf{B}}{2B}. \tag{A16}$$

Here we have made use of the condition $\nabla\cdot\mathbf{B}=0$ in the last step of Eq. (A15). Equation (A15) corresponds to the conservation of magnetic flux, $d(\sigma B)/ds = 0$, where σ is the cross section of a thin flux tube. And Eq. (A16) relates the average winding rate to the parallel current. For a force-free field satisfying $\nabla\times\mathbf{B}=\lambda\mathbf{B}$, Eq. (A16) can be further simplified as

$$\left\langle\frac{d\phi}{ds}\right\rangle = \frac{\lambda}{2}, \tag{A17}$$

and we have thus completed the derivation of Eq. (10). Heuristically, Eq. (A15) may be understood by consider a circular cross section of a radius r. The conservation of magnetic flux, $d(\sigma B)/ds = 0$, implies $\sigma^{-1}d\sigma/ds = -B^{-1}dB/ds$. Using this equation with the relation

$$\sigma^{-1}\frac{d\sigma}{ds} = \frac{1}{\pi r^2}\oint 2\pi r\frac{dr}{ds}d\phi = \left\langle\frac{2}{r}\frac{dr}{ds}\right\rangle, \tag{A18}$$

Eq. (A15) is obtained. Likewise, Eq. (A16) may be understood by considering a loop integral around the circular cross section and using the Stokes' theorem, which yields

$$\oint rB_\phi d\phi = 2\pi r\left\langle B_\phi\right\rangle = \pi r^2\mathbf{e}_3\cdot\nabla\times\mathbf{B}. \tag{A19}$$

Substituting Eq. (A19) in

$$\left\langle \frac{d\phi}{ds} \right\rangle = \frac{\langle B_\phi \rangle}{rB}, \tag{A20}$$

Eq. (A16) is recovered. Our derivation puts Eqs. (A15) and (A16) on a rigorous footing.

It is of great interest to consider the well-known Frenet-Serret comoving frame in conjunction with the present formulism. The Frenet-Serret frame is defined by the tangent vector $\bar{\mathbf{e}}_3 = d\mathbf{X}/ds$, the principal normal vector $\bar{\mathbf{e}}_1 = |d\bar{\mathbf{e}}_3/ds|^{-1}\,(d\bar{\mathbf{e}}_3/ds)$, and the binormal vector $\bar{\mathbf{e}}_2 = \bar{\mathbf{e}}_3 \times \bar{\mathbf{e}}_1$. These vectors satisfy the Frenet-Serret relations $d\bar{\mathbf{e}}_3/ds = \kappa\bar{\mathbf{e}}_1$, $d\bar{\mathbf{e}}_1/ds = -\kappa\bar{\mathbf{e}}_3 + \tau\bar{\mathbf{e}}_2$, and $d\bar{\mathbf{e}}_2/ds = -\tau\bar{\mathbf{e}}_1$, where κ is the curvature and τ is the torsion of the magnetic field line.[56] The Frenet-Serret relations can be expressed as

$$\frac{d}{ds}\bar{\mathbf{e}}_i = \bar{\boldsymbol{\omega}} \times \bar{\mathbf{e}}_i, \tag{A21}$$

with $\bar{\boldsymbol{\omega}} = \kappa\bar{\mathbf{e}}_2 + \tau\bar{\mathbf{e}}_3$. Because $\bar{\boldsymbol{\omega}} \cdot \bar{\mathbf{e}}_3 \neq 0$, the Frenet-Serret frame does not follow parallel transport. The angular velocity of the the Frenet-Serret frame, $\bar{\boldsymbol{\omega}}$, is related to the parallel transport angular velocity, $\boldsymbol{\omega}$, by $\bar{\boldsymbol{\omega}} = \boldsymbol{\omega} + \tau\mathbf{e}_3$. Therefore, the Frenet-Serret frame is rotating with respect to a parallelly transported comoving frame with an angular velocity $\tau\mathbf{e}_3$. If we instead measure the winding rate of a neighboring field line by the angle $\bar{\phi}$ with respect to $\bar{\mathbf{e}}_1$ of the Frenet-Serret frame, then

$$\frac{d\bar{\phi}}{ds} = \frac{d\phi}{ds} - \tau. \tag{A22}$$

In a toroidal device with its magnetic axis being a closed base field line, we are interested in the angle between the initial and final $\delta\mathbf{x}$ after a full toroidal circuit. The average of this angle over many circuits leads to the notion of rotational transform. To measure this angle, we need a reference frame that goes back to itself after a full circuit, a requirement that in general is not satisfied by a parallelly transported comoving frame. The Frenet-Serret frame, on the other hand, only depends on the local geometry of a curve, therefore is well-suited for the purpose. As such, the rotation angle after a full circuit can be expressed as a loop integral $\oint d\bar{\phi} = \oint d\phi - \oint \tau\, ds$, which has contributions from two parts. The first part, $\oint d\phi$, depends on the parallel current, as discussed above. However, the second part, $-\oint \tau\, ds$, only depends on the geometry of the magnetic axis. Consequently, a toroidal device can have a nonvanishing rotational transform even with a vacuum field, provided that the magnetic axis is nonplanar (therefore $\tau \neq 0$). This geometric angle is the basis of the figure-eight

and other stellarators with nonplanar axes. Interested readers are referred to Ref. [57] for further discussion.

---

[1] M. A. Raadu, Solar Physics **22**, 425 (1972).

[2] A. W. Hood, Plasma Phys. Control. Fusion **34**, 411 (1992).

[3] E. N. Parker, Astrophys. J. **174**, 499 (1972).

[4] Z. Mikić, D. D. Schnack, and G. van Hoven, Astrophys. J. **338**, 1148 (1989).

[5] K. Galsgaard and A. Nordlund, J. Geophy. Res. **101**, 13445 (1996).

[6] P. Dmitruk, D. O. Gómez, and E. E. DeLuca, Astrophys. J. **505**, 974 (1998).

[7] A. F. Rappazzo, R. B. Dahlburg, G. Einaudi, and M. Velli, Advances in Space Research **37**, 1335 (2006).

[8] A. F. Rappazzo, M. Velli, G. Einaudi, and R. B. Dahlburg, Astrophys. J. **657**, L47 (2007).

[9] A. F. Rappazzo, M. Velli, G. Einaudi, and R. B. Dahlburg, Astrophys. J. **677**, 1348 (2008).

[10] E. N. Parker, *Spontaneous Current Sheets in Magnetic Fields* (Oxford University Press, Inc., 1994).

[11] A. A. van Ballegooijen, Astrophys. J. **298**, 421 (1985).

[12] E. G. Zweibel and H.-S. Li, Astrophys. J. **312**, 423 (1987).

[13] S. K. Antiochos, Astrophys. J. **312**, 886 (1987).

[14] D. W. Longcope and H. R. Strauss, Astrophys. J. **437**, 851 (1994).

[15] C. S. Ng and A. Bhattacharjee, Phys. Plasmas **5**, 4028 (1998).

[16] A. W. Longbottom, G. J. Rickard, I. J. D. Craig, and A. D. Sneyd, Astrophys. J. **500**, 471 (1998).

[17] I. J. D. Craig and A. D. Sneyd, Solar Physics **232**, 41 (2005).

[18] S. I. Syrovatskii, Sov. Phys. JETP **33**, 933 (1971).

[19] M. N. Rosenbluth, R. Y. Dagazian, and P. H. Rutherford, Phys. Fluids **16**, 1894 (1973).

[20] E. R. Priest and M. A. Raadu, Solar Physics **43**, 177 (1975).

[21] S. I. Syrovatskii, Ann. Rev. Astron. Astrophys. **19**, 163 (1981).

[22] B. C. Low, Astrophys. J. **381**, 295 (1991).

[23] S. C. Cowley, D. W. Longcope, and R. N. Sudan, Physics Reports **283**, 227 (1997).

[24] R. A. Scheper and A. B. Hassam, Astrophys. J. **507**, 968 (1998).

[25] D. W. Longcope and S. C. Cowley, Phys. Plasmas **3**, 2885 (1996).

[26] A. L. Wilmot-Smith, G. Hornig, and D. I. Pontin, Astrophys. J. **696**, 1339 (2009).

[27] B. B. Kadomtsev, Fiz. Plasmy **1**, 710 (1975).

[28] H. R. Strauss, Phys. Fluids **19**, 134 (1976).

[29] J. J. Aly, Astron. Astrophys. **429**, 15 (2005).

[30] B. C. Low, Astrophys. J. **649**, 1064 (2006).

[31] B. C. Low, Phys. Plasmas **14**, 122904 (2007).

[32] A. M. Janse and B. C. Low, Astrophys. J. **690**, 1089 (2009).

[33] B. C. Low and Å. M. Janse, Astrophys. J. **696**, 821 (2009).

[34] Y.-M. Huang, A. Bhattacharjee, and E. G. Zweibel, Astrophys. J. Lett. **699**, L144 (2009).

[35] F. L. Waelbroeck, Phys. Fluids B **162**, 2372 (1989).

[36] Y.-M. Huang, E. G. Zweibel, and C. R. Sovinec, Phys. Plasmas **13**, 092102 (2006).

[37] E. G. Evstatiev, G. L. Delzanno, and J. M. Finn, Phys. Plasmas **13**, 072902 (2006).

[38] G. L. Delzanno, E. G. Evstatiev, and J. M. Finn, Phys. Plasmas **14**, 072902 (2007).

[39] V. A. Svidzinski, V. V. Mirnov, and H. Li, Phys. Plasmas **15**, 092106 (2008).

[40] E. N. Parker, Astrophys. J. **330**, 474 (1988).

[41] J. A. Klimchuk, Solar Physics **234**, 41 (2006).

[42] G. L. Delzanno, E. G. Evstatiev, and J. M. Finn, Phys. Plasmas **14**, 092901 (2007).

[43] Y.-M. Huang and E. G. Zweibel, Phys. Plasmas **16**, 042102 (2009).

[44] B. B. Kadomtsev and O. P. Pogutse, Sov. Phys. JETP **38**, 283 (1974).

[45] G. L. Delzanno and J. M. Finn, Phys. Plasmas **15**, 032904 (2008).

[46] R. Lionello, D. D. Schnack, G. Einaudi, and M. Velli, Phys. Plasmas **54**, 3722 (1998).

[47] R. Lionello, M. Velli, G. Einaudi, and Z. Mikić, Astrophys. J. **494**, 840 (1998).

[48] C. L. Gerrard and A. W. Hood, Solar Physics **214**, 151 (2003).

[49] C. L. Gerrard and A. W. Hood, Solar Physics **223**, 143 (2004).

[50] C. L. Gerrard, A. W. Hood, and D. S. Brown, Solar Physics **222**, 79 (2004).

[51] P. K. Browning, C. Gerrard, A. W. Hood, R. Kevis, and R. A. M. Van der Linden, Astron. Astrophys. **485**, 837 (2008).

[52] H. Grad, P. N. Hu, and D. C. Stevens, Proc. Natl. Acad. Sci. **72**, 3789 (1975).

[53] B. C. Low, private communication (2009).

[54] J. J. Aly and T. Amari, Astrophys. J. Lett. **709**, L99 (2010).

[55] I. J. D. Craig and A. D. Sneyd, Astrophys. J. **311**, 451 (1986).

[56] J. Mathews and R. L. Walker, *Mathematical Methods of Physics* (Addison-Wesley, Inc., 1970), 2nd ed.

[57] A. Bhattacharjee, G. M. Schreiber, and J. B. Taylor, Phys. Fluids B **4**, 2737 (1992).

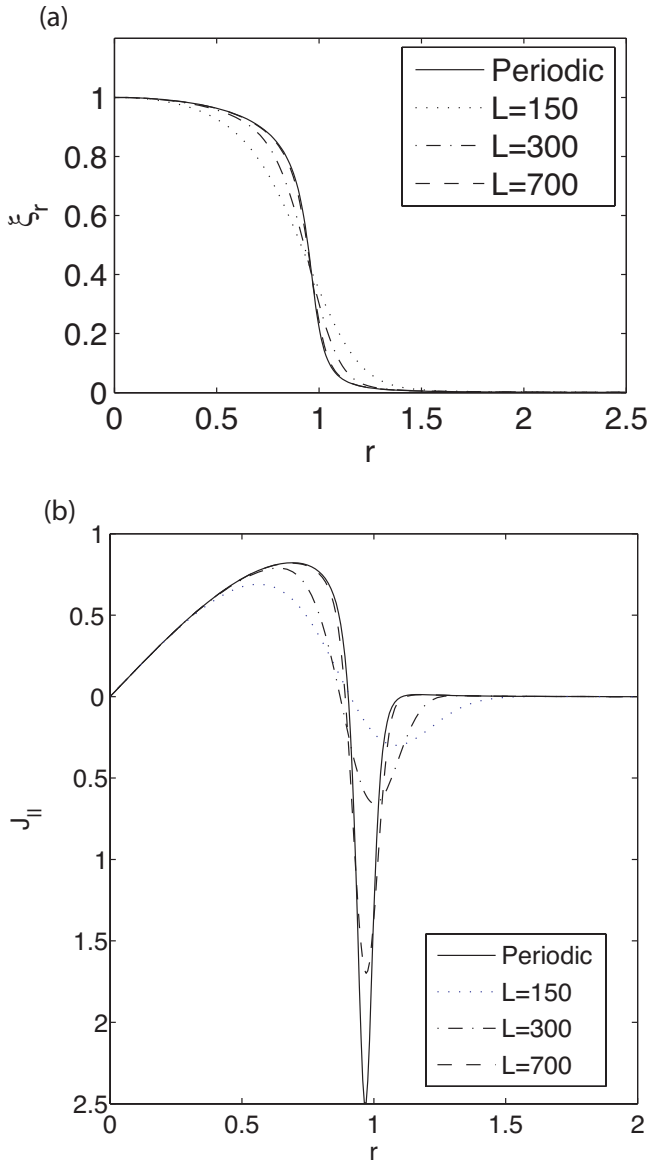

Figure 1: The radial displacement ξ_r and parallel current $J_{\|}$ of eigenmodes for different L, along the midplane $z = 0$. Also shown for comparison is the periodic case.

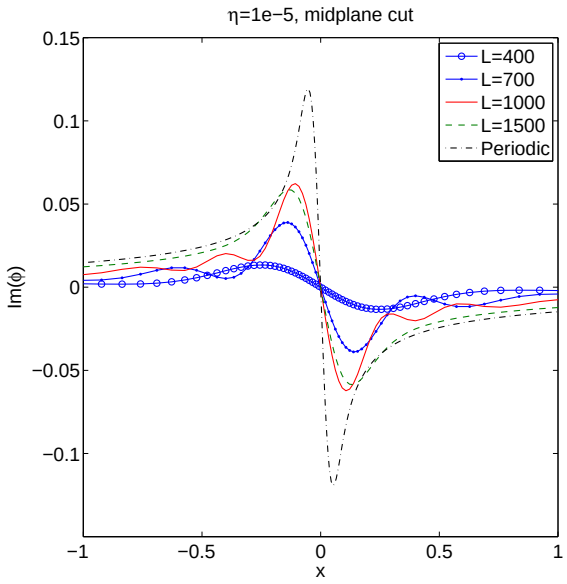

Figure 2: (Color online) The linear cut of the perturbed stream function $\tilde{\phi}$ along the mid-plane $z = 0$, for line-tied cases. Also shown for comparison is the periodic case with $k_z = 0$.